

Supporting Information for

Turn off the Majority-Rules Effect in Two-Dimensional Hierarchical Chiral Assembly by Introducing Chiral Mismatch

Shu-Ying Li,^{a,b} Ting Chen,^a Lin Wang,^{a,b} Dong Wang,^{*a} and Li-Jun Wan^{*a}

^a Key Laboratory of Molecular Nanostructure and Nanotechnology and Beijing National Laboratory for Molecular Sciences, Institute of Chemistry, Chinese Academy of Sciences (CAS), Beijing 100190, P.R. China

^b University of Chinese Academy of Sciences, Beijing 100049, P.R.China.

Contents:

1. STM images of the BIC-C6 and BIC-C16 honeycomb networks
2. Large-scale STM image of network II
3. Nonlinear chiral amplification in BIC-C10 assembly
4. Statistics based on the chirality of the trimer in monolayer
5. The specificity of hydrogen bonding interactions
6. Chiral communication in the assembly of BIC-C10 and (*R*)-2-octanol
7. Possible interdigitation modes between adjacent trimer for BIC-C6 or BIC-C16
8. Doping process in which the (*R*)-2-octanol is doped into the assembly of BIC-C10 and (*S*)-2-octanol
9. Doping process in which the (*S*)-2-octanol is doped into the assembly of BIC-C10 and (*R*)-2-octanol
10. Doping process in the assembly of BIC-C6 and BIC-C16
11. Adsorption energy from MM simulations
12. Experimental details

1. STM images of the BIC-C6 and BIC-C16 honeycomb networks.

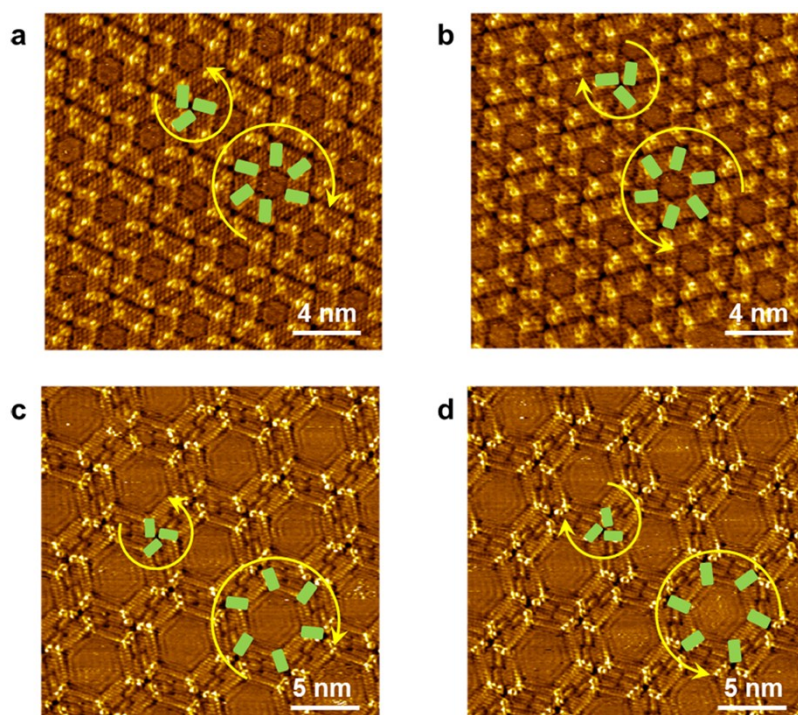


Figure S1. STM images of the BIC monolayers at the enantiopure chiral 2-octanol/HOPG interface. The trimer and hexamer in one domain rotate in opposite directions. (a) Honeycomb structure of BIC-C6 at the (*S*)-2-octanol/HOPG interface; (b) Honeycomb structure of BIC-C6 at the (*R*)-2-octanol/HOPG interface; (c) Honeycomb structure of BIC-C16 assembled from (*S*)-2-octanol; (d) Honeycomb structure of BIC-C16 assembled from (*R*)-2-octanol. Tunneling parameters: average tunneling current (I_{set}) = 0.5–1 nA, bias voltage (V_{bias}) = 900 mV. Green sticks outline the bright aromatic cores in BIC and are combined to indicate BIC trimer and hexamer in the assembly. Yellow arrows identify the handedness of the trimer and hexamer.

2. Large-scale STM image of network II.

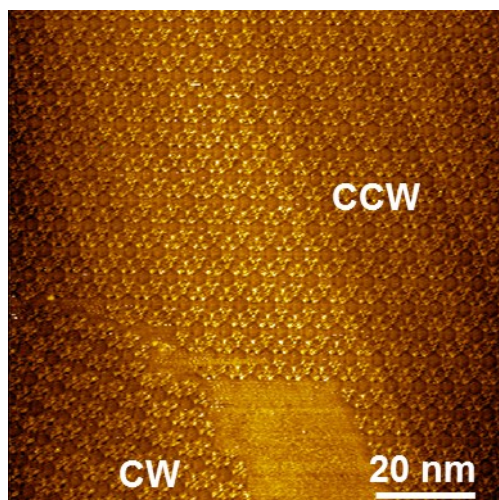


Figure S2. Large scale STM image of network II where CCW and CW enantiomeric motifs co-exist on the surface.

CW: CW hexamer network II; CCW: CCW hexamer network II.

3. Nonlinear chiral amplification in BIC-C10 assembly.

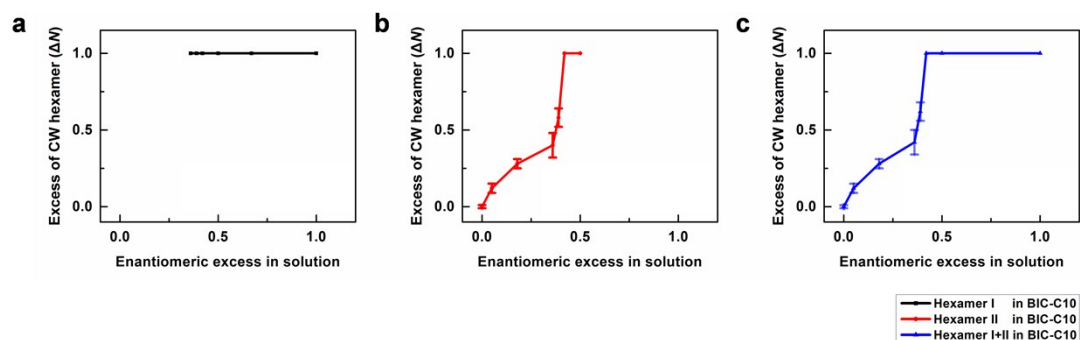


Figure S3. (a) Statistics based on network I; (b) Statistics based on network II; (c) Statistics based on the sum of network I and network II. Hexamer I+II means that we only look at the chirality of the trimer and hexamer, regardless of either network I or network II is formed. The ee in solution is defined as $ee = (S-R)/(S+R)$, in which R and S represent the amount of (R)-2-octanol and (S)-2-octanol in solution, respectively. For the organizational chirality, excess of one enantiomeric pattern is calculated according to $\Delta N = (N_1 - N_2)/(N_1 + N_2)$. The number of CW and CCW hexamer domains in STM images for one sample was summed up together and labeled as N_1 and N_2 , respectively.

4. Statistics based on the chirality of the trimer in monolayer

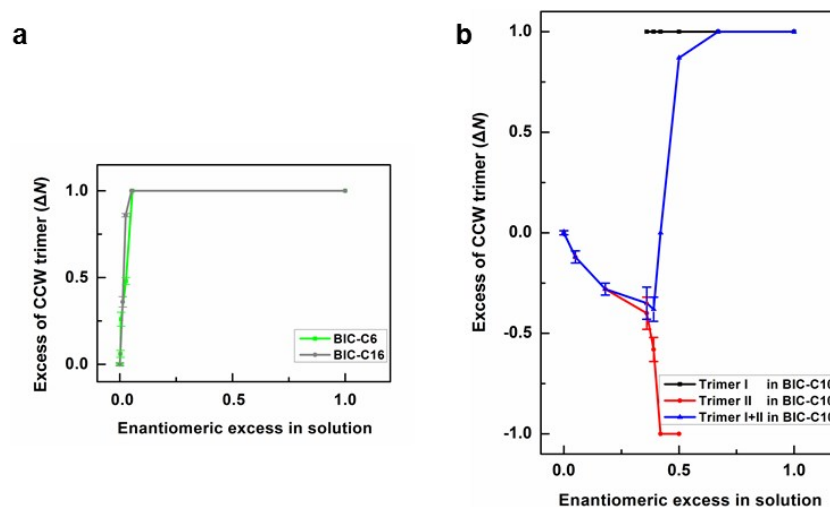


Figure S4. Nonlinear amplification of chirality in the assembly of BIC derivatives with an excess of (*S*)-2-octanol in solution. Statistics is based on the chirality of trimer. (a) Nonlinear amplification of chirality in BIC-C6 and BIC-C16 assemblies. Since the rotation directions of the trimer and hexamer in one domain of BIC-C6 or BIC-C16 are always opposite, statistics based on the chirality of trimer or hexamer are the same. (b) Statistics based on the rotational direction of the trimer in BIC-C10 assembly. Trimers I+II means that we only look at the chirality of the trimer, regardless of either network I or network II is formed. The enantiomeric excess (*ee*) in solution is defined as $ee = (S-R)/(S+R)$, in which *R* and *S* represent the amount of (*R*)-2-octanol and (*S*)-2-octanol in the solution, respectively. For the organizational chirality, excess of one enantiomeric pattern is calculated according to $\Delta N = (N_1 - N_2) / (N_1 + N_2)$. The number of CW and CCW hexamer domains in STM images for one sample was summed up together and labeled as N_1 and N_2 , respectively.

The organizational chirality excess of CCW trimer is plotted in Figure S4b. The curve goes negatively with the increase of *ee* of (*S*)-2-octanol. CW and CCW trimer domains of network II (red line in Figure S4b) co-exist on surface while only CCW trimer domain (black line in Figure S4b) can be observed in case of network I. The sum-up curves (blue curves in Figure S4b) are for statistics only.

5. The specificity of hydrogen bonding interactions

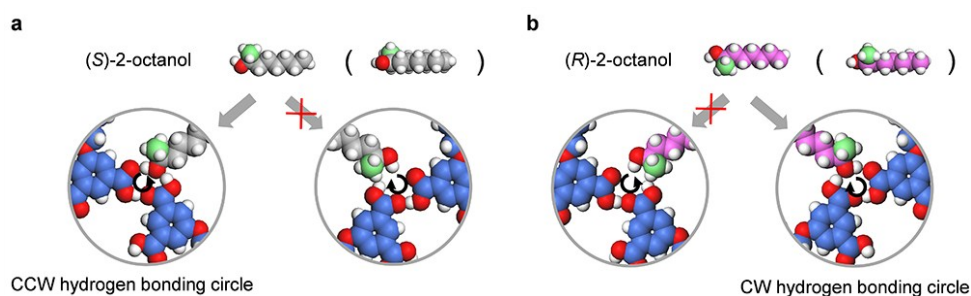


Figure S5. Molecular modeling for the conformational preference and the formation of directional hydrogen bondings. (a) Enantioselective adsorption conformation of (S)-2-octanol on surface and its corresponding CCW hydrogen bonding circle. (b) Enantioselective adsorption conformation of (R)-2-octanol and its corresponding CW hydrogen bonding circle. The arrow points to the direction of O-H...O hydrogen bond. For identification, S-enantiomer and R-enantiomer is painted gray and pink, respectively. Conformations in the brackets depict the side view of the enantiomers.

6. Chiral communication in the assembly of BIC-C10 and (R)-2-octanol

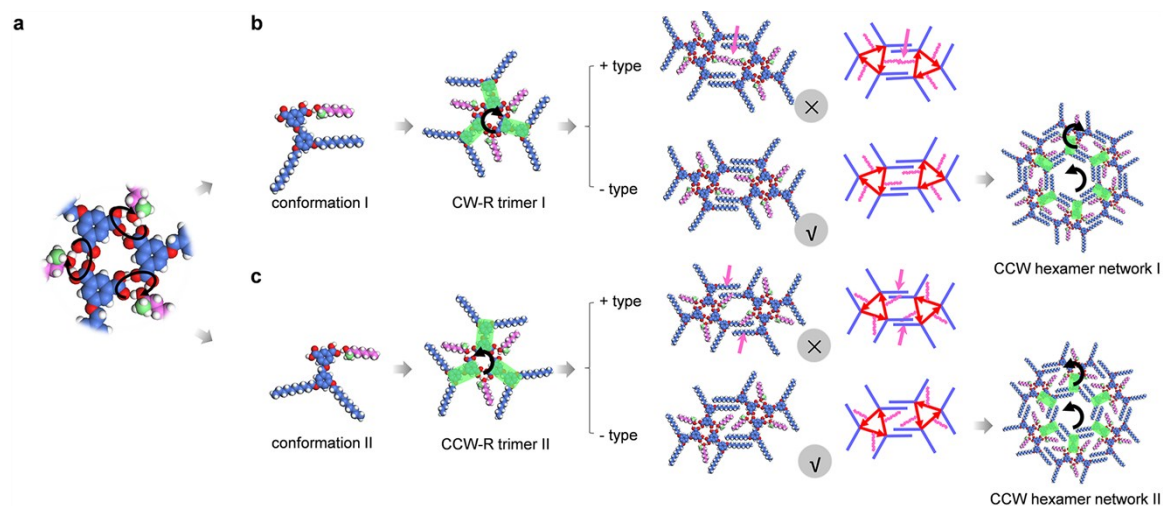


Figure S6. Illustration of the hierarchically chiral transmission from the chiral co-adsorber to the 2D assembly.

Co-assembly of BIC-C10 and (R)-2-octanol is demonstrated as a model system. (a) Intermolecular interactions

within a molecular trimer of BIC-C10 co-assembled with (*R*)-2-octanol. The black circle represents the 10-member hydrogen bonding ring composed of two carboxylic acid groups in adjacent BIC molecules and a hydroxyl group in (*R*)-2-octanol. The arrow points to the direction of O-H...O hydrogen bond. **(b)** Chiral transmission in network I. BIC molecules adsorb on surface in conformation I and constitute a CW trimer with (*R*)-2-octanol, which then interdigitates in - mode and assembles into CCW hexamer network I, which composed of CCW hexamers. **(c)** Chiral transmission in network II. The aromatic core at the bottom of the BIC molecule in conformation I flips horizontally around the C-O bond and this operation contributes to the formation of conformation II. BIC molecules adsorb on surface in conformation II and constitute a CCW trimer with (*R*)-2-octanol. As with the former situation, the CCW trimers still interdigitate in - manner and then further assemble into network II, which is also composed of CCW hexamers. To simplify the assembly process, the cartoon models are used, in which the red arrows denote the trimer chirality. For clear resolution, methyl groups are painted green and the (*R*)-2-octanol is colored pink. Aromatic cores are represented by green columns to help identifying the chirality of the trimer clearly. The ticks imply stable assembly structures while the crosses denote that the structures are unstable and the pink arrows point out the overlap of the alkyl chains. The rotation directions of the trimers and hexamers are indicated by the black arrows.

7. Possible interdigitation modes between adjacent trimers for BIC-C6 and BIC-C16, respectively

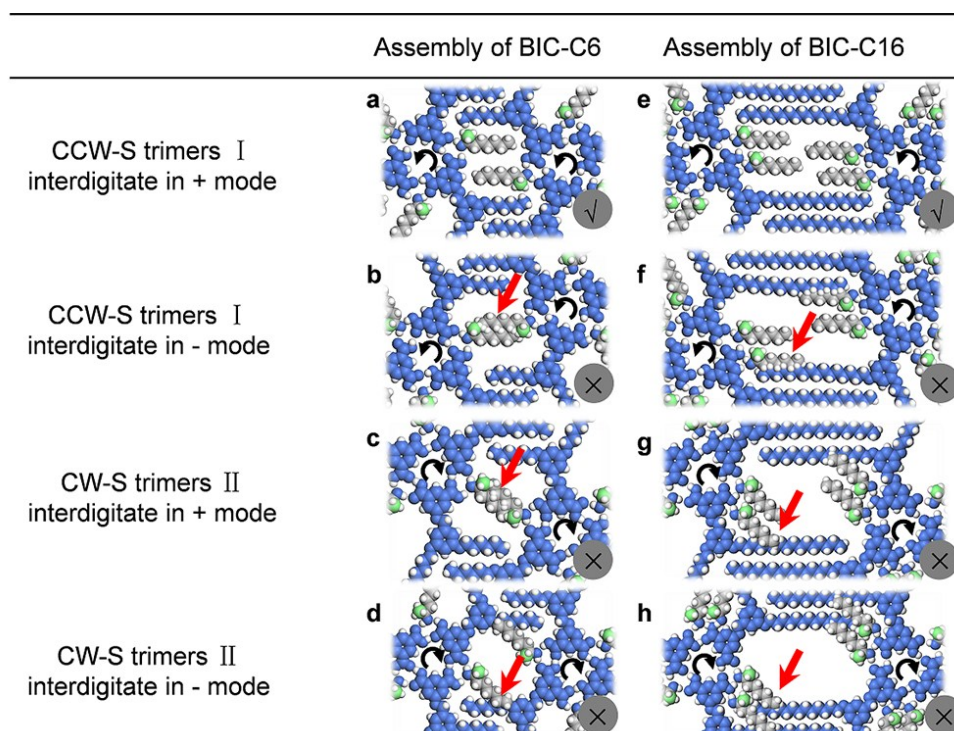


Figure S7. Possible interdigitation modes for BIC-C6 or BIC-C16 trimers at the enantiopure (*S*)-2-octanol/HOPG interface. (a) CCW-S trimers I of BIC-C6 interdigitate in + type; (b) CCW-S trimers I of BIC-C6 interdigitate in - type; (c) CW-S trimers II of BIC-C6 interdigitate in + type; (d) CW-S trimers II of BIC-C6 interdigitate in - type. (e) CCW-S trimers I of BIC-C16 interdigitate in + type; (f) CCW-S trimers I of BIC-C16 interdigitate in - type; (g) CW-S trimers II of BIC-C16 interdigitate in + type; (h) CW-S trimers II of BIC-C16 interdigitate in - type. Methyl groups are painted green. The co-adsorbed (*S*)-2-octanol is colored gray for identification. The ticks imply stable assembly structures while the crosses denote that the structures are unstable and the red arrows point out the intersections between alkyl chains which give rise to the adverse situation. The rotation directions of the trimers are displayed by black arrows.

8. Doping process in which (*R*)-2-octanol is doped into the assembly of BIC-C10 and (*S*)-2-octanol

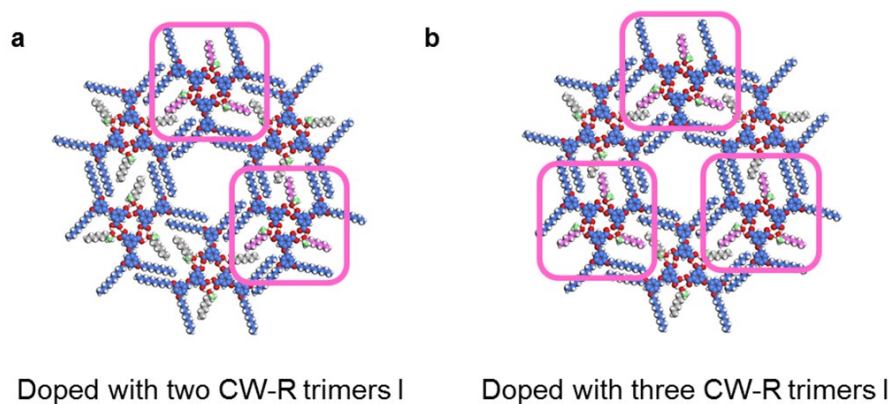


Figure S8. Incorporation of CW-R trimers I (formed by BIC-C10 and (*R*)-2-octanol) into a CW hexamer in network II (formed by BIC-C10 and (*S*)-2-octanol). (a) Incorporated two CW-R trimers I; (b) Incorporated three CW-R trimers I. For clarity, (*S*)-2-octanol are painted gray and the doped (*R*)-2-octanol is colored pink. The pink boxes outline the doping part in the hexagonal network.

9. Doping process in which (*S*)-2-octanol is doped into the assembly of BIC-C10 and (*R*)-2-octanol

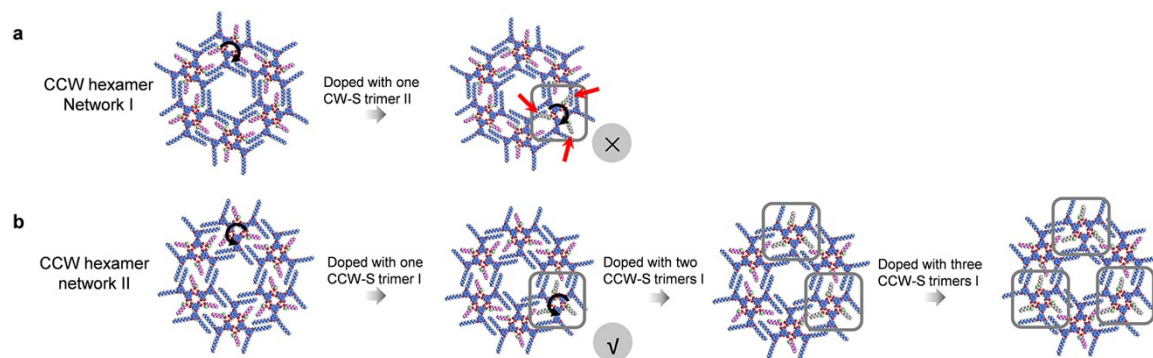


Figure S9. Illustration for doping the minority to the assembly of the majority. (a) Incorporation of a CW-S trimer II (formed by BIC-C10 and (*S*)-2-octanol) into the assembly of CCW network I (formed by BIC-C10 and (*R*)-2-octanol). The red arrows point out the intersections between alkyl chains which give rise to the adverse situation. (b) Gradual incorporation of CCW-S trimer I (formed by BIC-C10 and (*S*)-2-octanol) into the assembly of CCW

network II (formed by BIC-C10 and (*R*)-2-octanol). The ticks imply stable assembly structures while the crosses denote that the structures are unstable and the gray boxes outline the doping part in the hexagonal network. The rotation directions of the trimers are indicated by black arrows. For clarity, (*R*)-2-octanol is painted pink and the doped (*S*)-2-octanol is colored gray. It turns out that the CW-S trimer I can easily incorporate with the CCW hexamer network II composed of BIC-C10 and *R*-enantiomer, which contributes to the co-crystallization of *R*-enantiomer and *S*-enantiomer in mismatched structural units and consequently the inefficiency of chiral communication.

10. Doping process in the assembly of BIC-C6 and BIC-C16

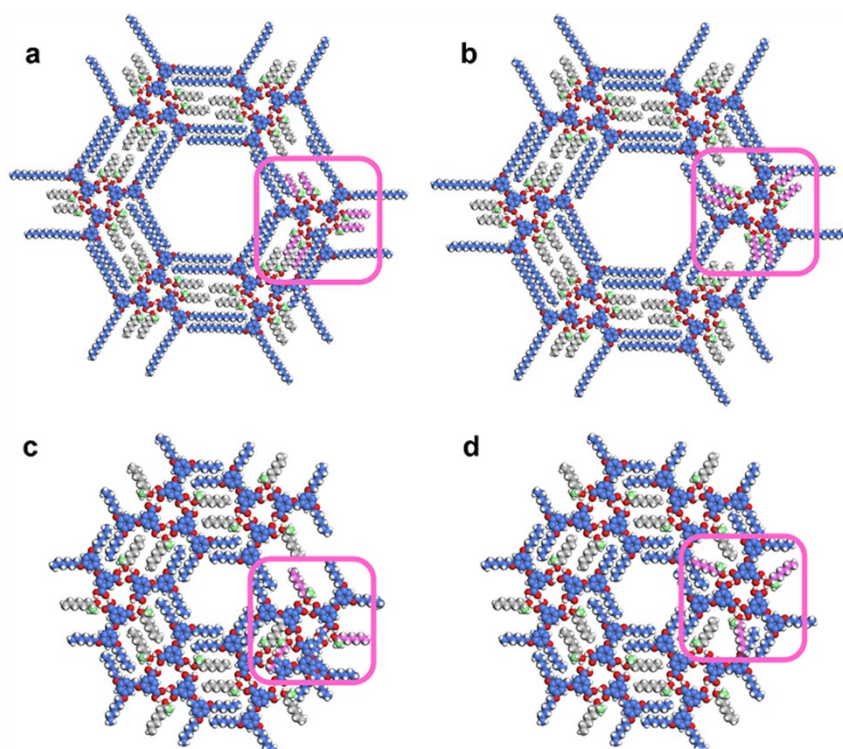


Figure S10. Illustration for the doping process in CW hexamer network I for BIC-C6 and BIC-C16, respectively.

Since only network I is able to be formed in the assembly of BIC-6 and BIC-C16, we performed the doping process in host honeycomb network regardless of network II in this case. (a) Incorporation of a CW-R trimer I (formed by BIC-C16 and (*R*)-2-octanol) into the assembly of network I (formed by BIC-C16 and (*S*)-2-octanol). (b)

Incorporation of CCW-R trimer II (formed by BIC-C16 and (*R*)-2-octanol) into the assembly of network II (formed by BIC-C16 and (*S*)-2-octanol). (c) Incorporation of a CW-R trimer I (formed by BIC-C6 and (*R*)-2-octanol) into the assembly of network I (formed by BIC-C6 and (*S*)-2-octanol). (d) Incorporation of CCW-R trimer II (formed by BIC-C6 and (*R*)-2-octanol) into the assembly of network II (formed by BIC-C6 and (*S*)-2-octanol). The doped (*R*)-2-octanol is colored pink and the methyl group at stereogenic center is painted green for identification. It turns out that serious overlap of the alkyl chains emerges in all of the cases (outlined by the pink boxes). And even an intact porous network cannot be formed in Supplementary Figure S5a and Supplementary Figure S5c, due to the mismatch between alkyl chains of neighboring trimers. Consequently, maintaining the consistency of the handedness of the trimers is necessary to fabricate a perfect porous network.

11. Adsorption energy from MM simulations

Table S1. Adsorption energy from MM simulations of the BIC hexagonal units linking with chiral co-adsorbers

	CW hexamer network I composed of S-OA	CW hexamer network II composed of S-OA	CW hexamer network II doped with one, two or three R-OA
Adsorption energy	-45.30	-44.86	-44.86

R-OA, (*R*)-2-octanol; S-OA, (*S*)-2-octanol. Adsorption energies are presented in kcal·mol⁻¹·nm².

12. Experimental details

BIC-C10 was synthesized as described in a previous report.¹ Chiral 2-octanol was used as solvent in this study and purchased from sigma-aldrich with purity of 99%. Concentration in all of the BIC solutions used in the present

study is all the same (1×10^{-4} M). To form self-assembled monolayers, a droplet of BIC solution was dropped onto a freshly cleaved HOPG (grade ZYB) surface. STM experiments were performed at the liquid/solid interface using PicoSPM (Agilent Technologies) in constant-current mode at room temperature. STM tips were mechanically cut from Pt/Ir wire (90/10). All STM images were shown without any modification.

Statistical methods. Distributions of the enantiomorphs of BIC-C6, BIC-C10 and BIC-C16 on surfaces were recorded based on at least three samples, respectively. For each sample, more than 20 large-scale STM images (100×100 nm²) were obtained at different locations.

Molecular simulations. 2D packing models of BIC were built according to the STM images. MM simulations were carried out with the molecular package TINKER using MMFF force field.²⁻⁴ The BIC monolayers are placed 0.35 nm above the upper layer of a two-layer sheet of graphite keeping the alkyl chains in BIC parallel to the directions of graphite symmetry axes. During optimization, the graphite was frozen. All simulations were carried out for the hexagonal structure consisted by six trimers containing three BIC molecules and three alcohols. Since the solvent molecules ((S)-2-octanol) are the same during simulation, the contribution of solvent in solution should be little to the adsorption energy of network I and network II when enantiopure solvent is applied. To reduce the calculated burden, the solvent molecules in solution are not considered during calculation. As processed in previous literature⁵, the calculated results from MM simulations are divided by the area possessed by the hexagonal network. Thus, the energy data provided in the text indicate the packing energy density in different networks. Adsorption energies are presented in kcal·mol⁻¹·nm⁻².

References

- 1 J. R. Gong, S. B. Lei, L. J. Wan, G. J. Deng, Q. H. Fan and C. L. Bai, *Chem. Mater.*, 2003, **15**, 3098-3104.
- 2 C. E. Kundrot, J. W. Ponder and F. M. Richards, *J. Comput. Chem.*, 1991, **12**, 402-409.

- 3 T. A. Halgren, *J. Comput. Chem.*, 1996, **17**, 490-519.
- 4 P. Ren, C. Wu and J. W. Ponder, *J. Chem. Theory Comput.*, 2011, **7**, 3143-3161.
- 5 C.-A. Palma, M. Bonini, A. Llanes-Pallas, T. Breiner, M. Prato, D. Bonifazi and P. Samorì, *Chem. Commun.*, 2008, 5289-5291.